

Electron-Cloud Simulation Results for the SPS and Recent Results for the LHC*

M. A. Furman and M. T. F. Pivi[†], LBNL, Berkeley, CA 94720, USA

July 11, 2002

Abstract

We present an update of computer simulation results for some features of the electron cloud at the Large Hadron Collider (LHC) and recent simulation results for the Super Proton Synchrotron (SPS). We focus on the sensitivity of the power deposition on the LHC beam screen to the emitted electron spectrum, which we study by means of a refined secondary electron (SE) emission model recently included in our simulation code.

1 Introduction.

The electron-cloud effect (ECE) is of considerable interest for the LHC, the main issue being the magnitude of the power deposition by the electrons on the vacuum chamber beam screen. A great deal of simulation work has been devoted to estimating the power deposition under various assumed conditions, in particular its sensitivity to the peak value δ_{\max} of the secondary emission yield (SEY) $\delta(E_0)$ of the copper layer of the beam screen, and its value at zero incident electron energy, $\delta(0)$ [1] (here E_0 is the incident electron energy).

For some time now we have been studying the ECE by means of multiparticle simulations with our code “POSINST” that includes a detailed probabilistic model of the secondary emission process [2]. Application of this simulation tool to the LHC [3] exhibited a strong sensitivity to the backscattered-electron and rediffused-electron components of the SEY, which dominate $\delta(0)$. This issue has attracted increased attention by recent measurements of the SEY at low energy for Cu [4] and other materials [5], that show values for $\delta(0)$ in the range $\sim 0.4 - 0.6$ [6, 7], which is significantly higher than earlier assumptions. One goal of this article is a better explanation of this sensitivity. For this purpose, we have carried out detailed fits of the SEY and the emitted-energy spectrum $d\delta/dE$ to particular sets of measurements for Cu and stainless steel (St.St.) [8]. A key, and fortuitous, feature of these sets of data is that the SEY curve for Cu is almost identical to that for St.St., as shown in Fig. 1, but that the secondary emission spectra is quite different, as seen in Fig. 2 for the case of 300 eV incident electron energy.

Our model takes into account the three main components of electron emission. Each of these components contributes an amount δ_i to the SEY, where $i = 1, 2, 3$ corresponds to true secondary, rediffused and backscattered electrons, respectively, so that $\delta = \delta_1 + \delta_2 + \delta_3$, where

$$\delta_i = \int_{E_i}^{E_{i+1}} dE \frac{d\delta}{dE} \quad (1)$$

For the data at $E_0 = 300$ eV shown in Fig. 1b, we set $E_1 = 0$, $E_2 = 50$ eV, $E_3 = 295$ eV, and $E_4 = 305$ eV (the value for E_2 of 50 eV is somewhat arbitrary, but conventional). Table 1 shows the three components as percentages of the total δ corresponding to this case. It is seen that $\delta_2 + \delta_3$ contributes substantially more to δ for St.St. than for Cu. These percentages vary with E_0 , although the general trend persists away from 300 eV. Our model does take this variation into account [8].

*Work supported by the US DOE under contract DE-AC03-76SF00098 and by the SNS project (ORNL). Proc. EPAC02, Paris, 3-7 June, 2002

[†]mafurman@lbl.gov and mpivi@lbl.gov

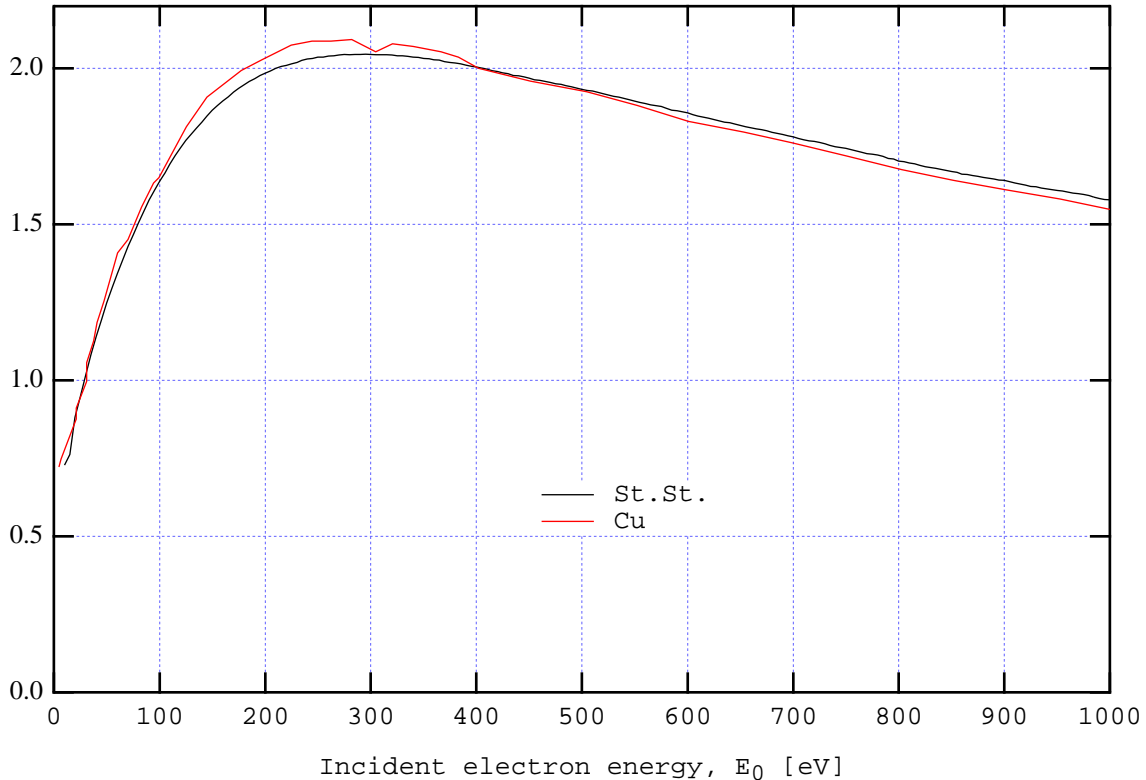


Figure 1: SEY at normal incidence as a function of incident electron energy for Cu (data courtesy N. Hilleret) and St.St. (data courtesy R. Kirby). The samples were measured by different apparatuses, and were in different states of surface conditioning.

We stress that the Cu and St.St. samples for which this data was taken were in different states of surface conditioning, and neither is representative of what is expected for the LHC beam screen in normal operation. In particular, the value $\delta_{\max} \simeq 2.05$ in this data is higher than what has been obtained by adequate conditioning of Cu samples of the LHC beam screen [4]. Of course, only the case of Cu is relevant to the LHC; we carry out here the simulation for both cases only for the purposes of exhibiting and explaining the sensitivity of the results to the details of the emitted energy spectrum.

We also present results for simulations for the SPS in a dipole magnetic field. As we are interested in benchmarking the code against measurements, we focus on the electron distribution, which exhibits characteristic peaks on either side of the center of the chamber.

2 Model.

In this article we consider only the dominant sources of electrons. For the LHC, the dominant source is the photoelectrons arising from the synchrotron radiation striking the walls of the vacuum chamber. For the

Table 1: Secondary components ($E_0 = 300$ eV).

	δ_1	δ_2	δ_3
Cu	84%	15%	1%
St.St.	57%	37%	6%

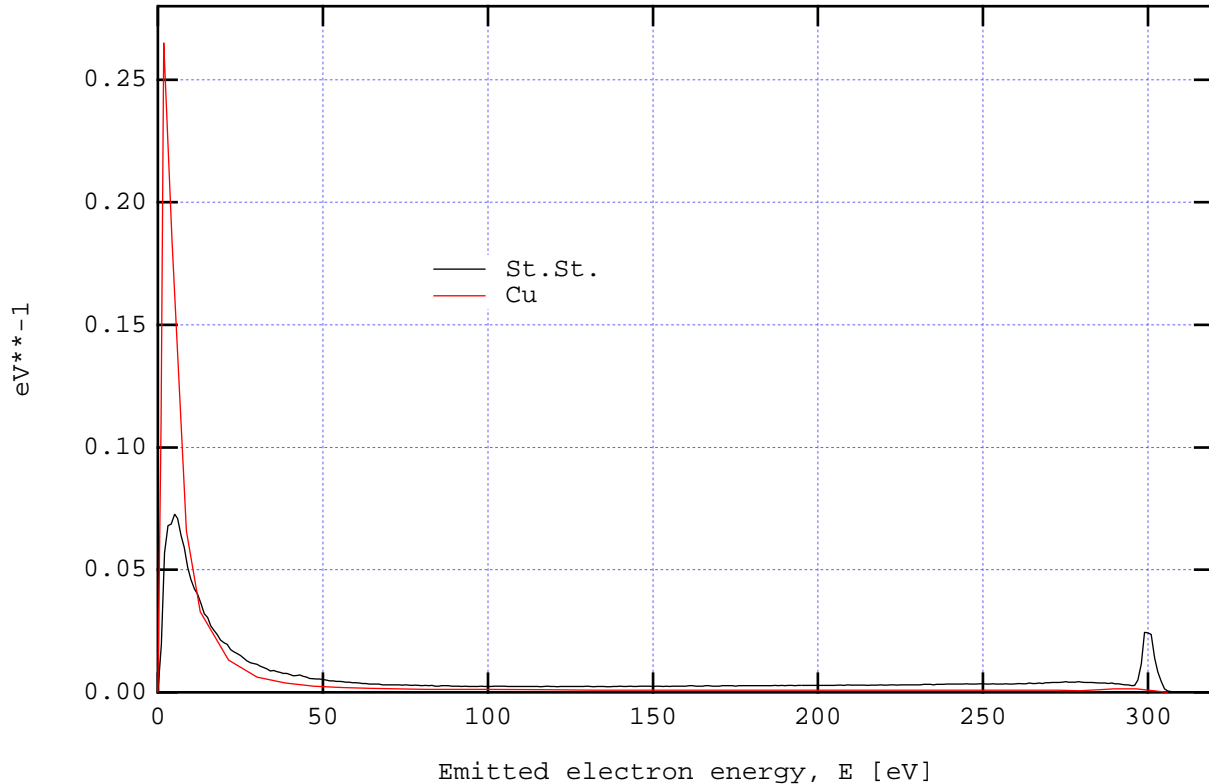


Figure 2: Secondary emission energy spectrum $d\delta/dE$ for 300 eV incident-electron energy for Cu (data courtesy N. Hilleret) and St.St. (data courtesy R. Kirby). The samples were measured by different apparatuses, and were in different states of surface conditioning.

SPS, it is electrons from ionization of the residual gas. In addition to these “seed electrons,” we consider the secondary electrons, emitted when the electrons strike the vacuum chamber walls under the action of successive bunch passages. Although our code accommodates other sources of electrons, we have turned them off for the purposes of this article.

For the simulation we take bunch length effects into account by dividing the bunch into a number of kicks N_k in the longitudinal direction. Space-charge forces of the electron cloud on itself are computed by means of a transverse grid, and are applied at every kick during the bunch passage and at every step during an empty bucket (empty buckets are divided up into N_e steps). The main parameters are specified in Table 2. Further details of the simulation are described in Ref. 3.

3 Power deposition in the LHC.

We have estimated the power deposited on the vacuum chamber of an LHC arc dipole by simulating a train of 50 bunches injected into an empty chamber followed by a 10-bunch long gap, for a total of $1.5 \mu\text{s}$ of beam time. We assume nominal parameters for the LHC bunch population and spacing, beam energy and beam sizes, listed in Table 2. We also assume a quantum efficiency per penetrated photon $Y' = 0.05$, and an effective photon reflection coefficient of 10%. This means that 90% of the photoelectrons are emitted on the outward “edge” of the chamber, where the synchrotron radiation strikes the chamber, and 10% uniformly around the rest of the chamber as a result of multiple photon reflections. The results for the instantaneous power deposition per unit length, $dE_a/dsdt$, are shown in Figs. 3 and 4 in units of J/m/s (here E_a is the energy absorbed by the wall). Preliminary results were presented in Ref. 9.

The average power deposition in steady state (time interval $0.5 \leq t \leq 1.2 \mu\text{s}$ in Figs. 3 and 4) are 152

Table 2: Assumed parameters for the SPS and LHC.

Parameter	Symbol	SPS	LHC
Proton beam energy	E , GeV	26	7000
Dipole field	B , T	0.2	8.4
Bunch population	$N_p \times 10^{11}$	0.8	1.05
Bunch spacing	τ_g , ns	25	25
Bunch length rms	σ_z , cm	30	7.7
Trans. bunch size	σ_x, σ_y , mm	3, 2.3	0.3, 0.3
Pipe semi-axes	a, b , mm	77, 22.5	22, 18
Kicks/bunch	N_k	101	51
Steps/empty bucket	N_e	25	41
Photon reflectivity	R	-	10%
Quantum efficiency	Y'	0	0.05
Peak SEY	δ_{\max}	1.9	2.05
Peak SEY energy	E_{\max} , eV	260	270
Sp. charge grid size	h_x, h_y , mm	7.7, 2.25	2.5, 2.5

W/m for St.St. and 11 W/m for Cu. In addition to these two cases, we computed a third case in which we artificially eliminated the rediffused and backscattered components of the emitted spectrum, retaining only the true secondary electrons, and rescaled the SEY to $\delta_{\max} = 2.05$. In this case, the average power deposition is 2.1 W/m. If we average $dE_a/dsdt$ over the whole run ($0 \leq t \leq 1.5 \mu\text{s}$ in Figs. 3 and 4), the average power deposition is roughly half of the above-quoted values. Fig. 5 shows a detail of Fig. 4. The origin of this large sensitivity is explained in Sec. 5 below. We note that our simulations show a strong time dependence of the power deposition, with instantaneous values reaching ~ 100 W/m for copper, and ~ 30 W/m for copper without backscattered or rediffused electrons. These large values obtain for ~ 5 ns after the passage of a bunch, and last for a few ns.

4 SPS simulation.

In the case of the SPS, we are primarily interested in reproducing a feature of the electron-cloud spatial structure, namely the position of the “vertical stripes,” or regions of high electron density, which appear in the presence of a dipole magnetic field. The vertical stripes are reproduced by the simulations, as seen in Fig. 11, which shows a histogram of the horizontal projection of the time-averaged electron cloud density (simulation parameters are listed in Tab. 2). In this case, the results are quite similar for Cu and St.St., showing stripes at $\sim \pm 18$ mm, in agreement with CERN simulations [10], and in disagreement with the measured location at $\sim \pm 9$ mm [11]. The peaks at ± 2 mm in Fig. 11 are mostly due to an artifact of our time-averaging procedure; indeed, instantaneous snapshots of the distribution show these peaks much reduced.

5 Conclusions.

The large sensitivity of the power deposition in the LHC chamber to the composition of the emitted-energy spectrum can be explained as follows: When an electron strikes the chamber it is much more likely to emit high-energy secondaries when the rediffused plus backscattered component is large, as in the case of St.St., than when it is small, as for Cu. Consequently, as the electrons “rattle around” the chamber during the inter-bunch gap, the average electron-wall collision energy degrades more slowly for St.St. than for Cu. The fastest energy degradation, of course, occurs when the rediffused plus backscattered SEY components are neglected altogether. This effect can be seen in our simulation results shown in Figs. 6 and 7. The variation in the energy degradation translates into a corresponding trend in the effective SEY, as seen in Figs. 8 and

9, which, in turn, is reflected in the average line density of the electron cloud (Fig. 10). Further details will be presented in a future publication [12].

We emphasize that our estimated value for the electron-cloud power deposition, computed in Sec. 3 for $\delta_{\max} = 2.05$, is significantly larger than what can realistically be expected once the Cu surface of the beam screen becomes sensibly conditioned, whereupon a value $\delta_{\max} = 1.3$ may be achieved [13]. Our results underscore the need for reliable data on the SEY and emitted-energy spectrum in order to improve the estimate of the magnitude of the power deposition in the LHC.

Our simulations show a strong time dependence of the power deposition, with instantaneous values reaching ~ 100 W/m for copper, and ~ 30 W/m for the copper model without backscattered nor rediffused electrons. These large values, which obtain for ~ 5 ns after the passage of a bunch and last for a few ns, might impact the design of the beam screen cooling system.

For the SPS dipole simulation, the agreement between the simulated stripe locations with experiment is off by a factor of ~ 2 . We do not at present have an explanation for this discrepancy, which merits further investigation.

6 Acknowledgments.

We are indebted to R. Kirby and N. Hilleret for supplying us with data and many discussions. We are grateful to I. Collins, R. Cimino and F. Zimmermann for valuable discussions. We are grateful to NERSC for supercomputer support.

References

- [1] For an updated summary and links to other electron-cloud sites, see the Proc. E-CLOUD02, CERN, 15-18 April 2002, <http://slap.cern.ch/collective/ecloud02/>, particularly the talks by F. Zimmermann, G. Rumolo and M. Furman.
- [2] M. A. Furman and G. R. Lambertson, Proc. MBI-97 Workshop, KEK, 15-18 July 1997; KEK Proceedings 97-17, Dec. 1997 (Y. H. Chin, ed.), p. 170.
- [3] M. A. Furman, LBNL-41482/CBP Note 247/LHC Project Report 180, May 20, 1998.
- [4] V. Baglin, I. Collins, B. Henrist, N. Hilleret and G. Vorlaufer, LHC Project Report 472, 2 August 2001.
- [5] R. E. Kirby and F. K. King, SLAC-PUB-8212, October 2000.
- [6] F. Zimmermann, Proc. XI Chamonix Workshop, Jan. 2001, <http://cern.web.cern.ch/CERN/Divisions/SL/publications/chamx2001/contents.html>
- [7] M. A. Furman and M. Pivi, Proc. PAC01, Chicago, June 18-22, 2001, p. 1898.
- [8] M. A. Furman and M. Pivi, LBNL-49711, CBP Note-415, June 2002, to be submitted for publication.
- [9] M. A. Furman, Ref. 1.
- [10] F. Zimmermann, Ref. 1.
- [11] J. M. Jiménez *et al.*, Ref. 1.
- [12] M. Furman and M. Pivi, to be published.
- [13] N. Hilleret, Ref. 1.

Disclaimer.

This document was prepared as an account of work sponsored by the United States Government. While this document is believed to contain correct information, neither the United States Government nor any agency thereof, nor The Regents of the University of California, nor any of their employees, makes any warranty, express or implied, or assumes any legal responsibility for the accuracy, completeness, or usefulness of any information, apparatus, product, or process disclosed, or represents that its use would not infringe privately owned rights. Reference herein to any specific commercial product, process, or service by its trade name, trademark, manufacturer, or otherwise, does not necessarily constitute or imply its endorsement, recommendation, or favoring by the United States Government or any agency thereof, or The Regents of the University of California. The views and opinions of authors expressed herein do not necessarily state or reflect those of the United States Government or any agency thereof, or The Regents of the University of California.

Ernest Orlando Lawrence Berkeley National Laboratory is an equal opportunity employer.

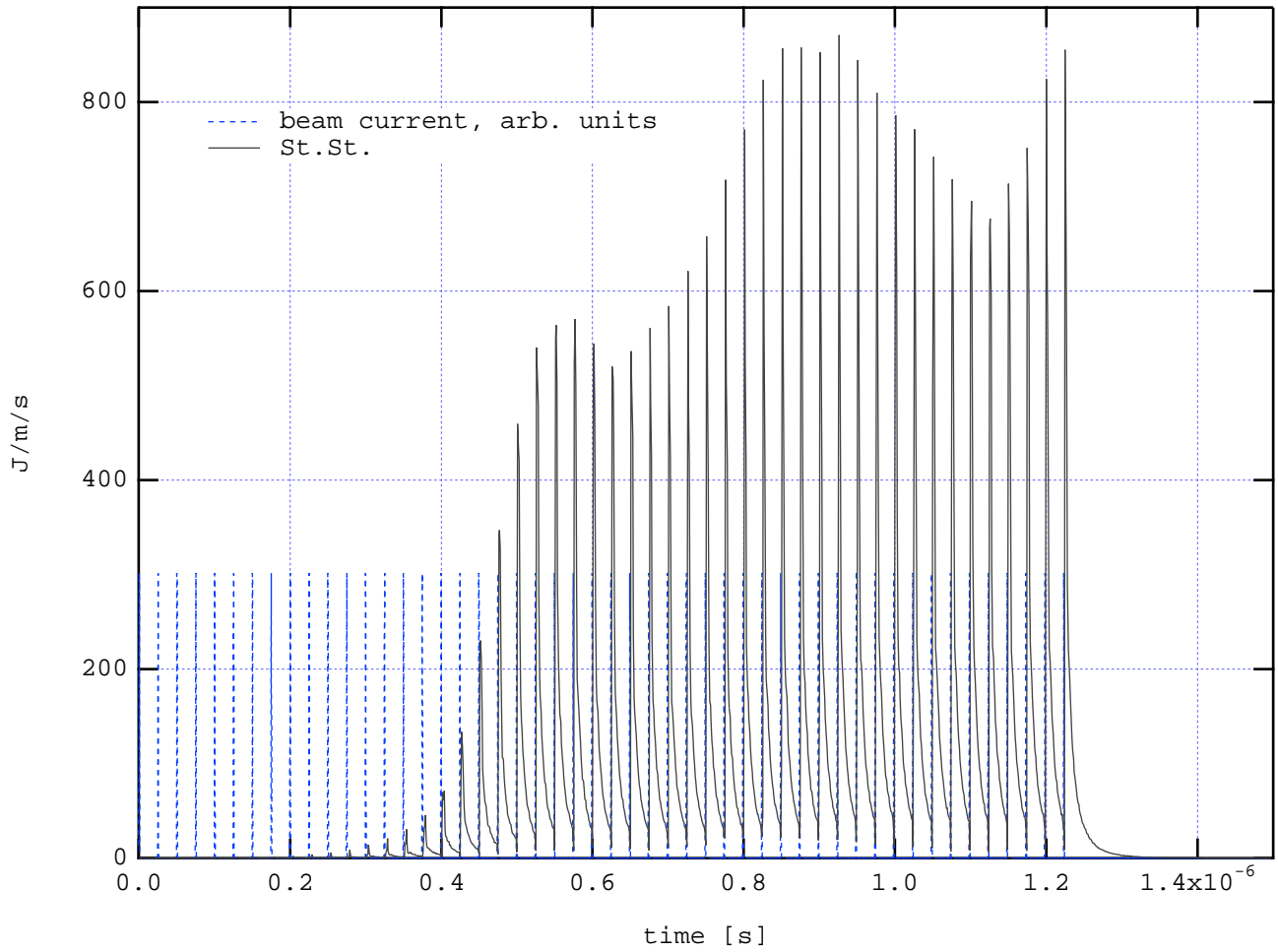


Figure 3: Simulated instantaneous electron-cloud power deposition in an LHC arc dipole assuming a St.St. model for the secondary emission process at the surface of the beam screen (see text).

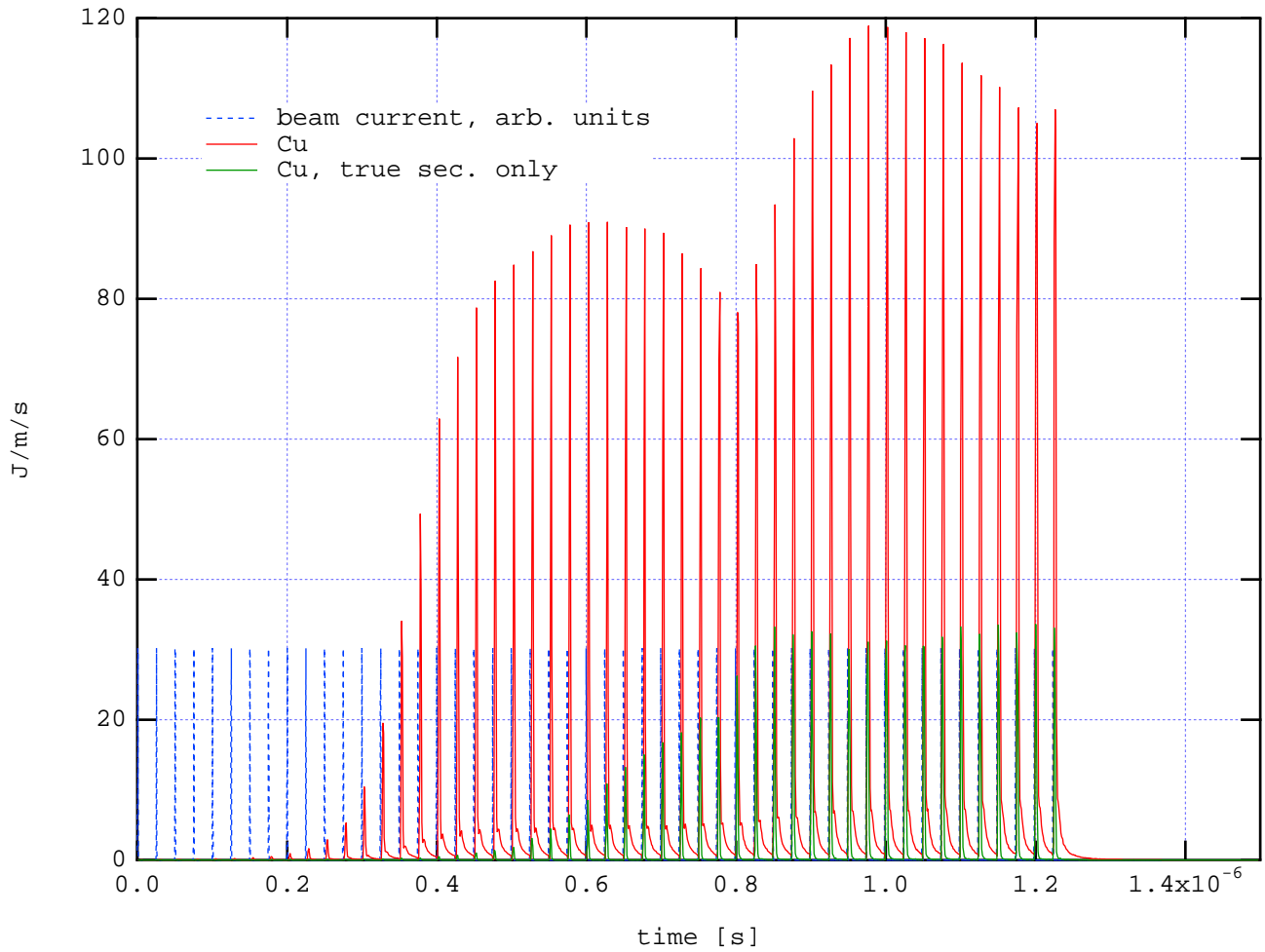


Figure 4: Simulated instantaneous electron-cloud power deposition in an LHC arc dipole assuming a Cu model for the secondary emission process at the surface, and for a Cu model in which only the true secondary emission is considered (see text). Note that the vertical scale is $\sim 13\%$ of Fig. 3.

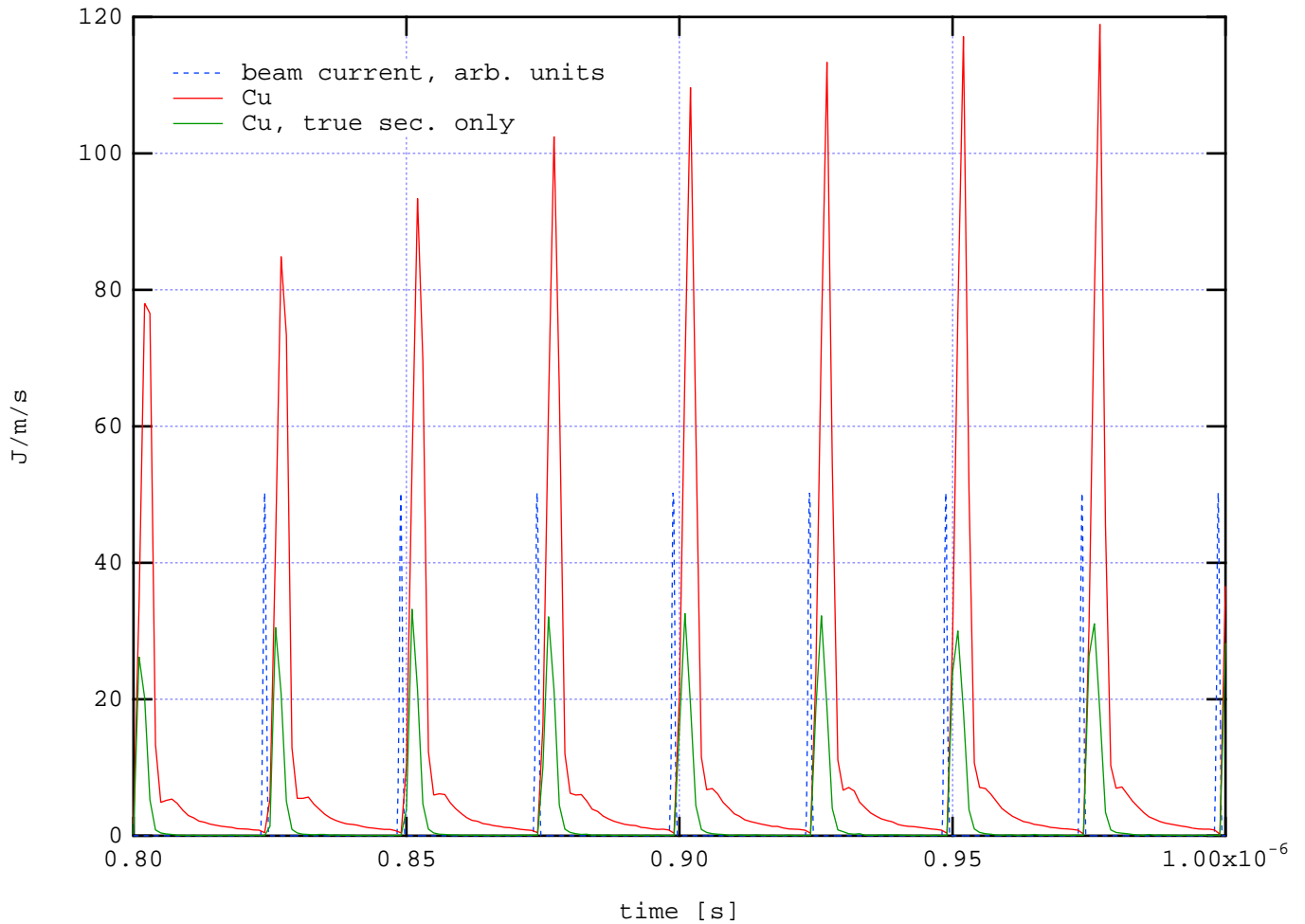


Figure 5: Detail of Fig. 4. Note that, for the case in which only true secondary electrons are considered, the power deposition falls very quickly during the inter-bunch gap owing to the fast dissipation of the electron cloud.

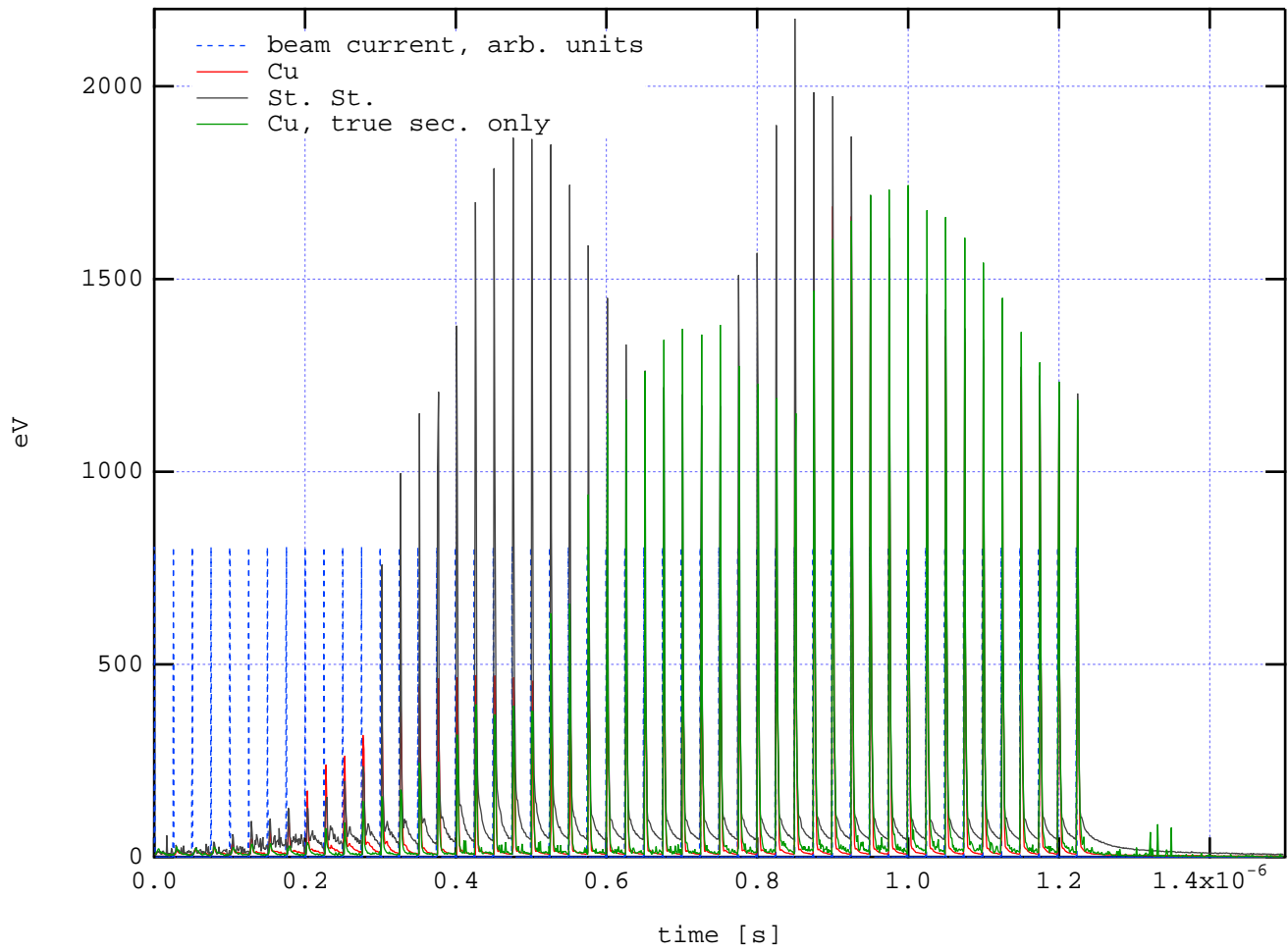


Figure 6: Simulation results for the average electron-wall collision energy.

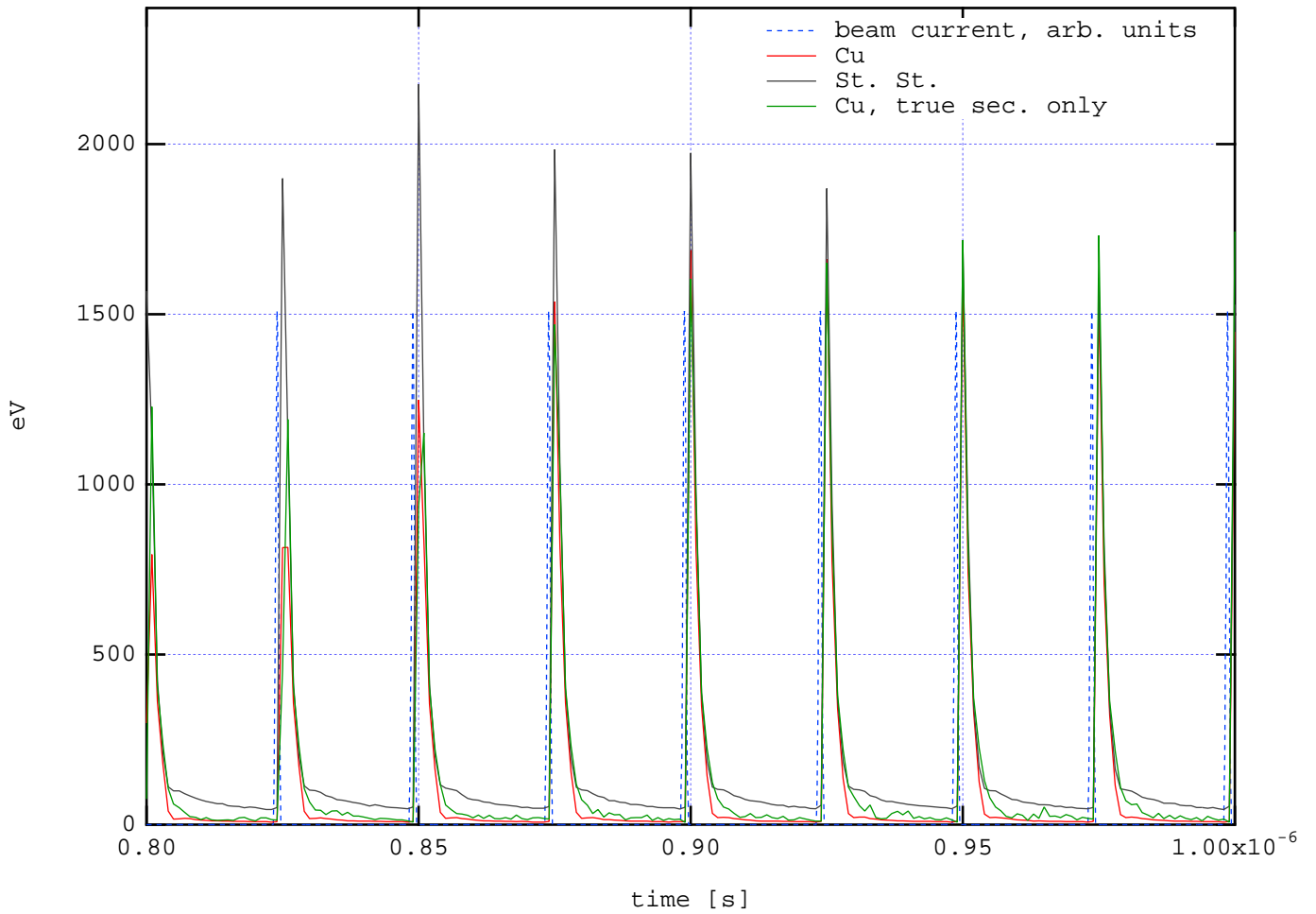


Figure 7: Detail of Fig. 6. Note that, during the interbunch gap, the electron energy degrades more slowly for St.St. than for Cu owing to the larger rediffused and backscattered components.

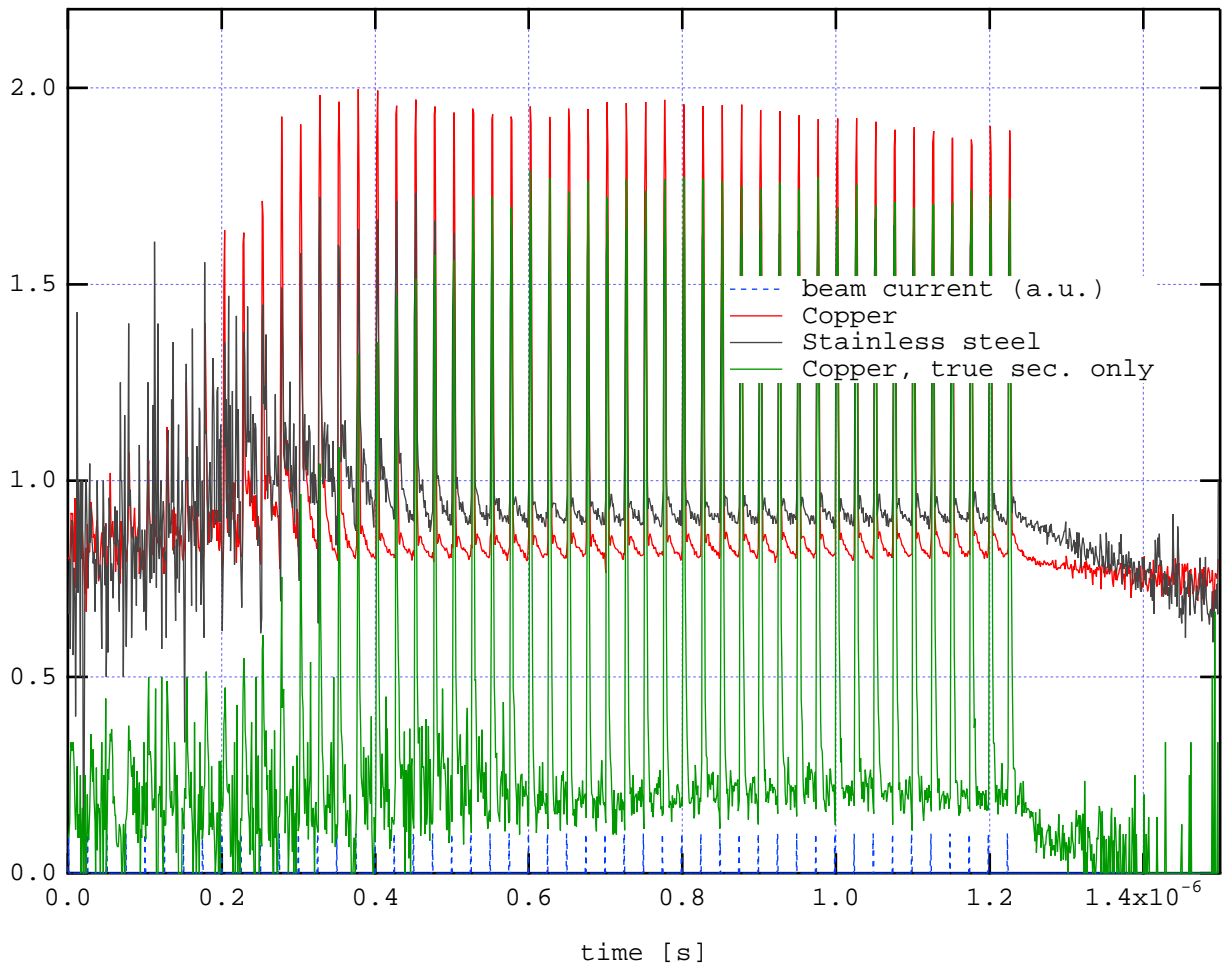


Figure 8: Simulation results for the effective secondary emission yield.

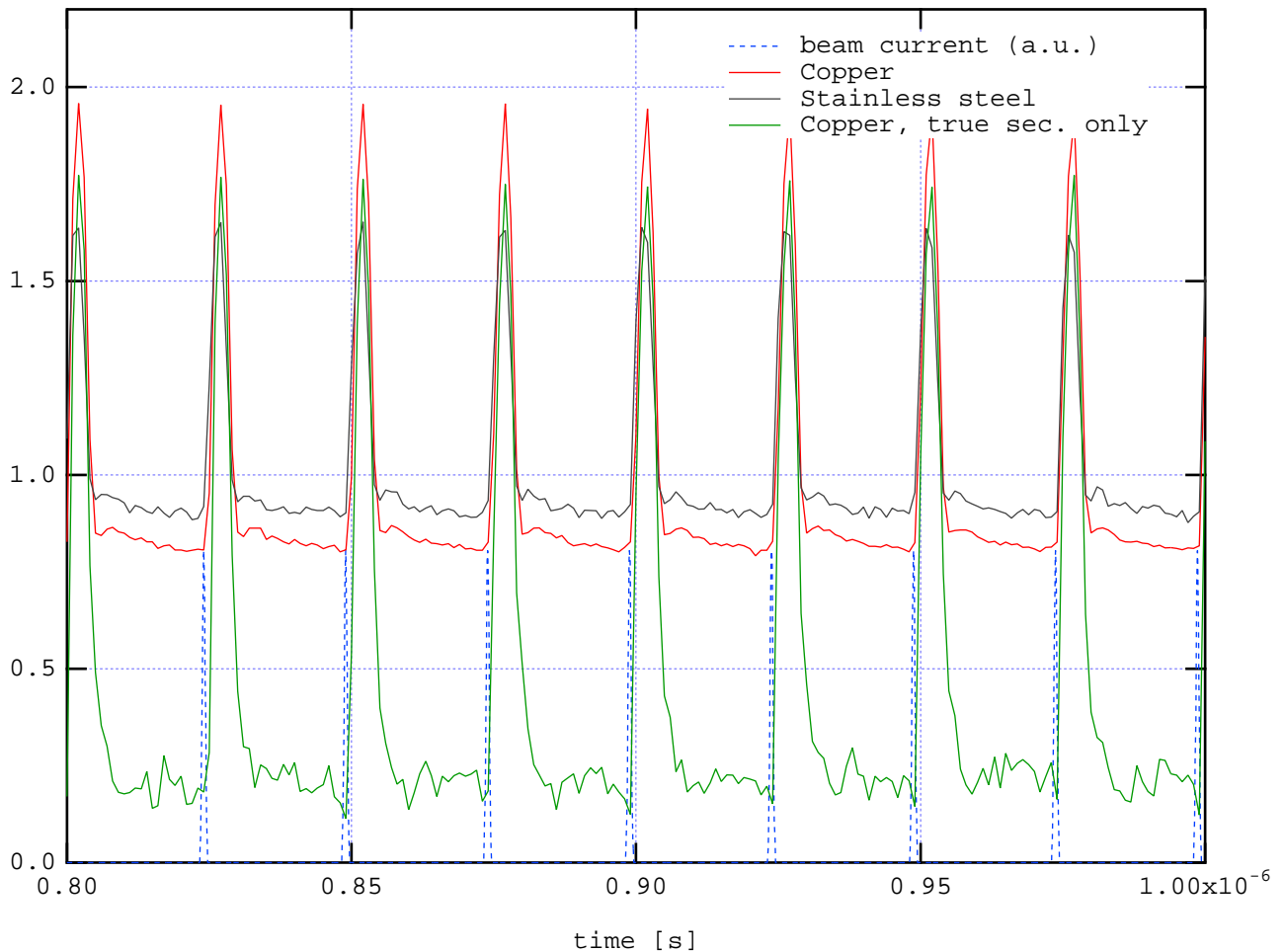


Figure 9: Detail of Fig. 8. Note that the SEY reaches high values for all three models ~ 5 ns following the passage of any given bunch. This high value is determined by the energy acquired by the electrons following the bunch, typically ~ 1500 eV peak value, for which the SEY is roughly the same for all three models. However, during the inter-bunch gap, as the electrons “rattle around” the chamber, their energy degrades and the effective yield decreases, and is smaller for Cu than for St.St., and even smaller when only true secondary electrons are considered.

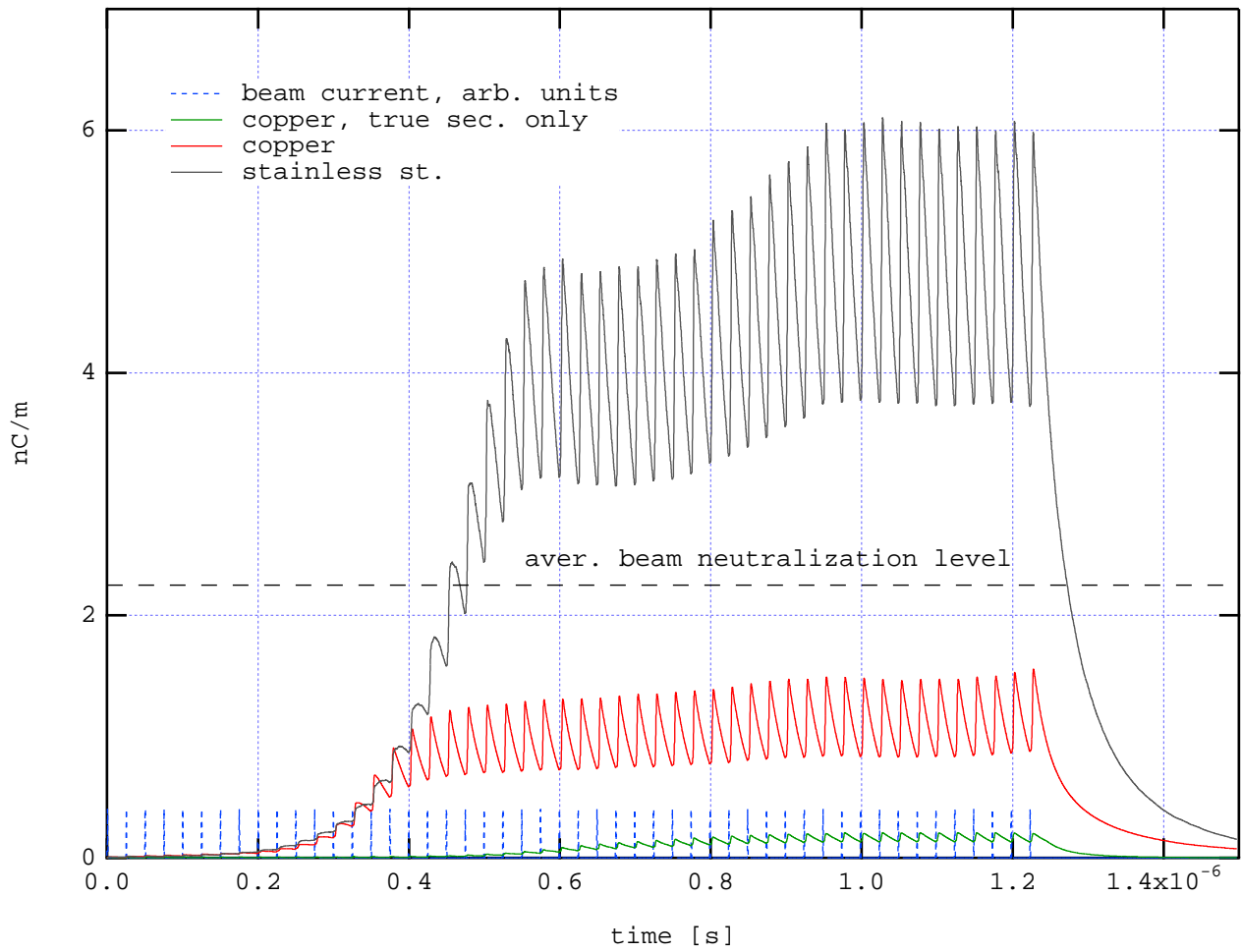


Figure 10: Average electron-cloud line density in the chamber.

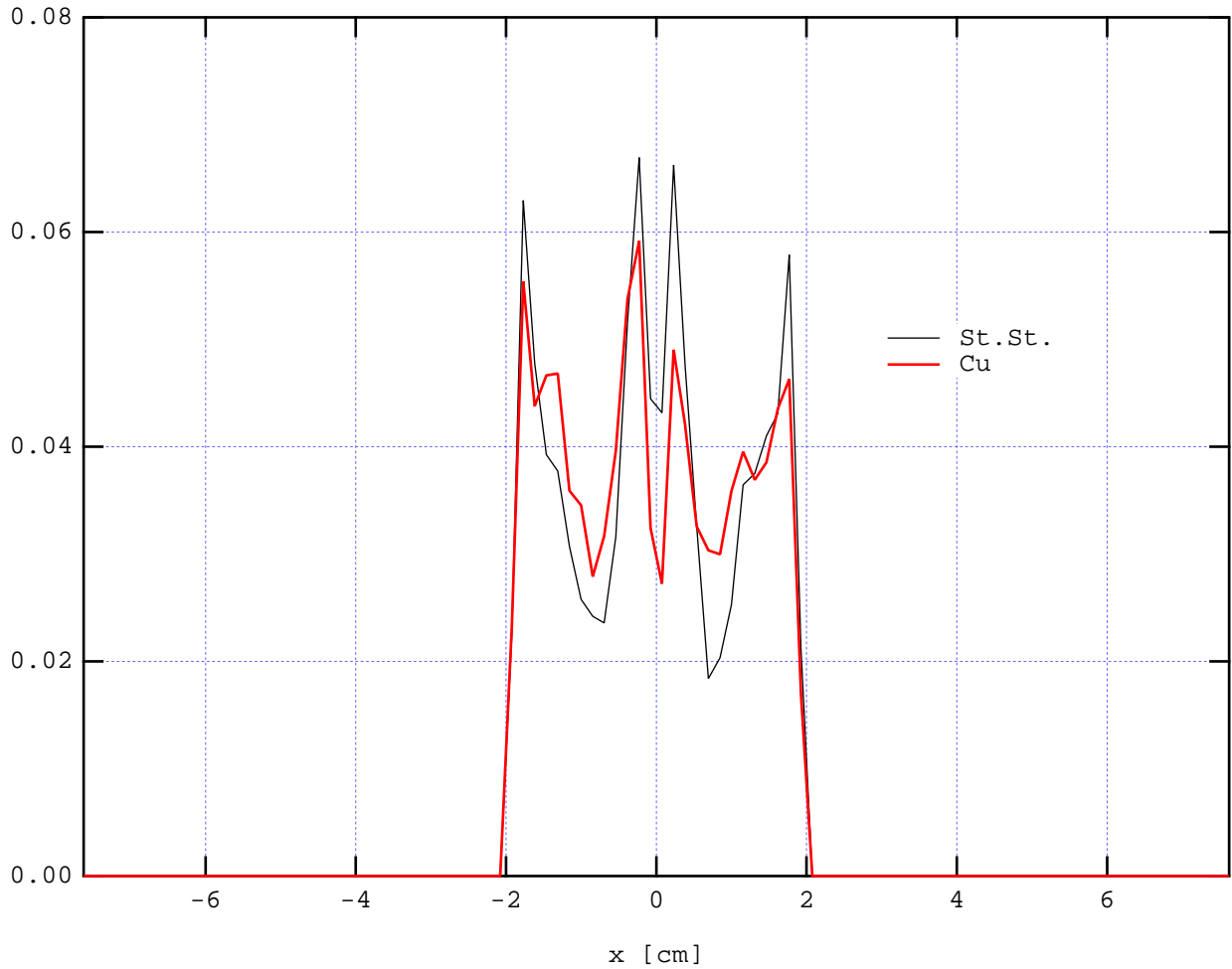


Figure 11: Histogram of the horizontal projection of the time-averaged electron-cloud density in a dipole magnet at the SPS. Although the electron density is quite different for Cu and St.St, we have normalized the two histograms to unity in order to emphasize the similarities of the distributions.